Ionic Liquid Conditioning of Poly(vinylferrocene) for the Doping/Undoping of Glycylglycylglycine Tripeptide

Yijun Tang,[†] Gary A. Baker,[‡] and Xiangqun Zeng*,[†]

The Department of Chemistry, Oakland University, Rochester, Michigan 48309, and Chemical Sciences Division, Oak Ridge National Laboratory, Oak Ridge, Tennessee 37831

Received: April 4, 2010; Revised Manuscript Received: June 3, 2010

Potentiodynamic electrochemical measurements of the redox-driven entry and exit of ionized glycylglycylglycine peptide (GGG^-) during polymer oxidation and reduction, respectively, are presented and interpreted for electroactive poly(vinylferrocene) (PVF)-modified electrodes. Frequently, electrochemically controlled redox cycling results in the dramatic alteration in polymer film properties, typically accompanied by loss of redox activity, exemplified in this case by negligible currents associated with repeated exposure to GGG. Notably, we have discovered that preconditioning of PVF films with suitable ionic liquids (ILs) such as the *N*-alkyl-*N*-methylpyrrolidinium bis(trifluoromethanesulfonyl)imides allows the electroactive film to relax to a state compatible with reversible GGG^- doping/undoping. Our studies substantiate that both the cation and the anion of the IL must be considered as both play important roles in appropriately conditioning the PVF polymer films. Indeed, ILs with structures and properties highly divergent from the target GGG^- failed to properly condition PVF to a compatible state.

1. Introduction

Electroactive polymer-modified electrodes have garnered great attention since their initial discovery in the late 1970s. An excellent account of the early activity in this area was published in 1984.[1] One of the attractive properties of conductive polymer-modified electrodes is that counterions must transport into and out from the polymer matrix in order to balance excessive charges caused by the oxidation/reduction of electroactive centers. This drive toward electroneutrality provides a potential means for the redox-modulated transport and uptake/release of species with applications in (bio)analytical sensors, energy transduction materials, electromechanical actuators, molecular immobilization supports, and electrochromic devices.[2,3] By varying the electrode potential, mobile species in the bathing electrolyte can be either doped in or released from the polymer matrix;[4] however, the dynamic transport of species into/out of the polymer films is complex, involving not only electron transport and coupled ion transport but also the solvent transfer and polymer reconfiguration. The structure of conductive polymer can be categorized at three levels.[5] The first level is the basic chemical composition. The nature of the monomer unit(s) will determine the general behavior of the conductive polymer. The second level of structure involves the spatial arrangement of the basic conductive polymer units within the individual conductive polymer molecules (the microstructure). This is determined to a great extent by the polymerization reaction and the precise doping conditions. The morphology and the interior structure of the polymer after it is modified onto an electrode are often rigid, lacking the desired flexibility. This limits the practical use of conductive polymers to reversibly release doped species unless the polymer matrix is specifically tuned to accommodate the species of interest. Typically, only small ions can be reversibly doped into and released from conductive polymers under potential control. The third level of the structure is the spatial arrangement of the conductive polymer chains in the solid state (the macrostructure). Wegner[6] pointed out that conducting polymers have a salt structure when prepared by (electro) chemical oxidation or reduction of neutral precursors. The salt structure consists of two sublattices, one of which is formed from segments of the polymer chain carrying a positive or negative charge. The other sublattice is formed by (doped) counterions, which maintain the overall electrical neutrality of the system. Changes in conductive polymer properties must be intimately linked to changes in the doped counterion's sublattice and polymer structures. We hypothesize that ionic liquids (ILs) can play roles as both solvent and electrolyte to fine-tune conductive polymer structures after they are coated onto the substrate electrodes to expand the range of species amenable to redox-controlled catch and release. ILs have a number of unique attributes that suggest this may be possible. First, ILs are an attractive solvent choice from a green chemistry standpoint.[7] Second, interactions between ILs and polymers are predominantly electrostatic and van der Waals in nature. Additionally, the large and bulky charged ions of ILs interact with each other via directional electrostatic interactions. These molecular interactions can be used to maximize the polymer relaxation process so that the polymer can be tuned to the optimum configuration for transporting species of interest after IL treatment.[8] Third, there are many varieties of ILs available such that the selection can in principle be optimally tailored to the species of interest.[9] To test this hypothesis, we compared the doping and dedoping processes for the glycylglycylglycine anion (GGG^-) for PVF-modified electrodes before and after conditioning using a range of ILs. PVF was selected as a fundamental system for modeling redox conductive polymer systems for its high stability and because it comprises localized one-electron redox centers bonded to the polymer backbone. The electrochemical properties of PVF films have also been explored previously in various electrolytes including aqueous solutions of inorganic/organic salts,[10] organic solutions,[11] IL

* To whom correspondence should be addressed.
[†] Oakland University.
[‡] Oak Ridge National Laboratory.

10.1021/jp1030202
Published on Web 07/26/2010

solutions, and pure IL.[8] The characterization of PVF-modified electrodes in aqueous solutions containing small biomolecules such as amino acids has also been reported.[12] These studies revealed that the redox activity of PVF films was irreversibly altered by the doping of larger counterions. In the current work, we have selected GGG^- as a relatively large counterion to investigate the tunability of PVF-modified electrodes conditioned using ILs. This tripeptide is composed of three glycine units and has a simple rod shape. Because glycine has an isoelectric point of 6.0, in aqueous solution GGG is expected to be partially ionized (GGG^-). We note that GGG has a distinguished history of use as a model compound or standard reference in studying metal−peptide interactions.[13,14] GGG^-, which can be safely assumed to retain the geometry known for GGG, can thus be doped into oxidized PVF films. Since there are no reports on the behavior of PVF films in peptide-containing electrolytes, characterizing the redox activity of PVF-modified electrodes in GGG solution assumes fundamental importance. In this paper, we will demonstrate that conditioning PVF films with ILs bearing some structural similarity to GGG facilitates polymer reconfiguration for the doping/undoping of GGG^-, resulting in significantly improved reversibility.

2. Experimental Section

2.1. Materials. Poly(vinylferrocene) (PVF, MW ≈ 50 000, cat. no. 09746) was purchased from Polysciences, Inc.; tetrabutylammonium perchlorate (TBAP, cat. no. 394) was purchased from GFS Chemicals; dichloromethane (CH_2Cl_2, cat. no. 61005-0040) was purchased from Acros Organics; sodium perchlorate ($NaClO_4$, cat. no. S1513) and 1-*n*-butyl-3-methylimidazolium tetrafluoroborate ([BMIM][BF_4]) (cat cat. no. 91508) were purchased from Sigma-Aldrich. All other ILs were synthesized and purified following methods established previously,[15−17] including *N*,*N*-methyl-*n*-butylpyrrolidinium bis(trifluoromethanesulfonyl)imide ([C_4pmy][Tf_2N]), *N*,*N*-methyl-*n*-pentylpyrrolidinium bis(trifluoromethanesulfonyl)imide ([C_5mpy][Tf_2N]), tripropyl-*n*-hexylammonium bis(trifluoromethanesulfonyl)imide ([N_{3336}][Tf_2N]), 1-*n*-butyl-3-*n*-butylimidazolium hexafluorophosphate ([BBIM][PF_6]), tetraoctylammonium bis(2-ethylhexyl)sulfosuccinate ([N_{8888}][AOT]), and 1-*n*-butyl-3-methylimidazolium bis(pentafluoroethylsulfonyl)imide ([BMIM][beti]). Glycylglycylglycine (GGG, cat. no. G13770) was purchased for Sigma-Aldrich. The 10-MHz Au quartz crystal electrodes were purchased from the International Crystal Manufacturing Company (Oklahoma City). Aqueous solutions used in this study contained 0.1 M $NaClO_4$ and 0.05 M GGG.

2.2. Cast-Coated PVF Films. Methylene chloride solution containing 0.1 M PVF was drop cast onto the surface of gold electrodes. After the solvent evaporated, a PVF film was obtained on the gold surface. The estimated amount of PVF deposited was about 0.026 g/cm^2.

2.3. Electrooxidatively Coated PVF Films. Electrooxidatively deposited PVF films were cast onto a gold electrode from a dichloromethane solution that contained 0.1 M TBAP and 2.5 mM PVF.[18] In this case, the gold electrode used was a 10-MHz AT-cut quartz crystal Au electrode. A potential of 0.7 V was applied to the gold electrode and held for 3 min, followed by stepping to 0 V with another 3 min hold. This potential step cycle was repeated three times in total. Finally, 0.7 V was applied to the gold electrode for 3 min before the electrode was disconnected from the potentiostat. This treatment procedure resulted in precipitation of an oxidized PVF film onto the gold-coated electrode. The PVF-modified electrode was rinsed with deionized water and dried in air for at least 24 h prior to use. All potentials reported in this work are with respect to the saturated calomel electrode (SCE), unless noted otherwise.

2.4. Potentiostat and EQCM Measurements. One technique commonly used to probe redox-driven changes of polymer-modified electrodes is the electrochemical quartz crystal microbalance (EQCM), in which electrochemical measurement is performed concurrently with quartz crystal microbalance (QCM) measurement. In our setup, a Bi-Potentiostat (Pine Instrument Co., Model AFRDE5) was used for the electrochemical analysis and a Research Quartz Crystal Microbalance (RQCM, Maxtek, Inc.) was used to monitor the resonance frequency changes for the PVF-coated QCM electrode. The values of potential, current, charge, quartz resonance frequency, and the damping resistance of the equivalent Butterworth-van Dyke (BVD) circuit[19] were recorded at a rate of 20 points per second. The data were exported through the RQCM A/D port to a PC with a Windows 98 operating system for further analysis. A single-compartment cell was used with a PVF-coated QCM gold electrode mounted on the side. The QCM gold disk electrode, which faced the electrolyte solution, was used as the working electrode. A platinum wire served as counter electrode and a SCE was used as the reference electrode.

2.5. AFM Imaging. Atomic force microscopy (AFM) images were obtained with a PicoPlus System (Molecular Imaging, Tempe, Arizona). The cantilever used was a silicon nitride probe from BudgetSensors (Sofia, Bulgaria) with a resonant frequency of 30 kHz and a force constant of 0.27 N/m.

2.6. ATR-FTIR Spectroscopy. The FT-IR spectra were obtained with a Varian 3100 FT-IR Excalibur Series spectrometer, using a ZeSe attenuated total reflectance (ATR) accessory from Specac (Cranston, Rhode Island).

3. Results and Discussions

PVF-modified electrodes can be made either by simple drop casting from solution or by electrooxidative coating. Figure 1 compares the polymer film surface morphologies achieved for PVF films cast-coated and electrooxidatively coated at gold surfaces. Drop casting, while a simpler approach, was found to result in the growth of distinct islands. Because electrooxidative coating produced a far more continuous PVF film on the gold electrode, this approach was followed in the remainder of the work reported herein.

3.1. GGG^- Doping/Dedoping. Cyclic voltammetry (CV) was performed on a PVF-coated gold electrode in the presence of 0.1 M $NaClO_4$ and 0.05 M GGG. No buffer was used in making GGG stocks in order to avoid the introduction of superfluous ions. The aqueous solution of GGG showed a pH of 6. That suggests that a large fraction of GGG was likely present in zwitterionic form with a smaller population existing as GGG^-. Although electooxidatively coated PVF showed reversible and reproducible perchlorate doping/undoping, PVF films exposed to GGG^- showed little redox activity (Figure 2); therefore, as-produced these PVF films have little potential in the transport of GGG because of difficult doping/undoping and/or low mobility of GGG^- in the aqueous solution.

As discussed in our earlier work,[8] CV of PVF-coated electrodes in pure IL shows a slow break-in effect, indicating dynamic polymer film relaxation and conformation changes under the influence of potential perturbation. The IL−polymer interactions at open circuit conditions allow the PVF to relax to its equilibrium or steady state situation and can completely eliminate this break-in effect. Furthermore, neutral ILs are doped into the PVF film at 0 V. During the PVF oxidation process, the doping of counterions is accompanied by the removal of

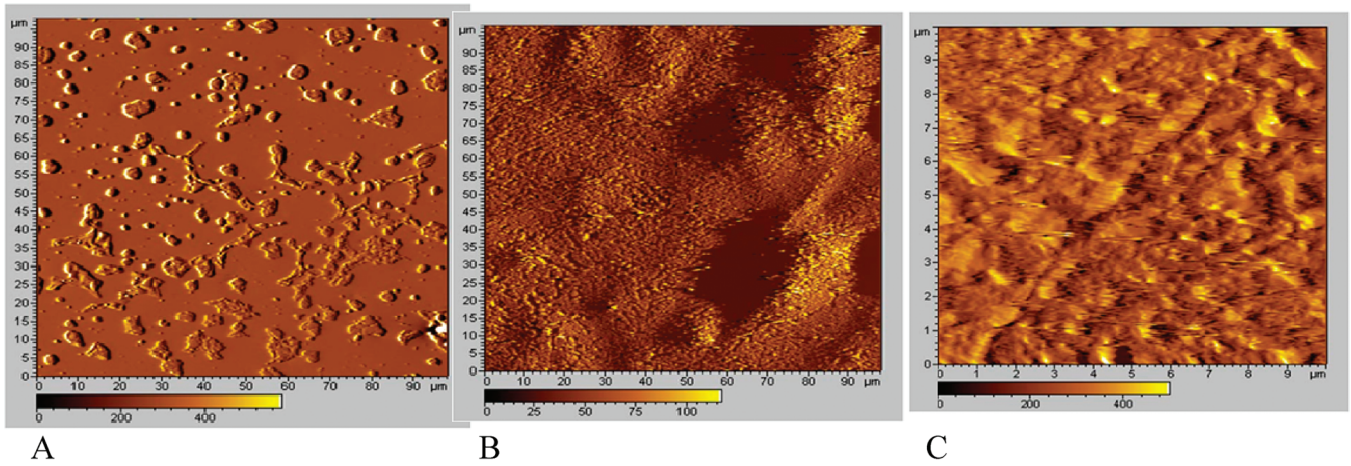

Figure 1. Contact mode AFM images of PVF films on a gold surface: (A) cast-coated PVF, 100 × 100 μm; (B) electrooxidatively coated PVF, 100 × 100 μm; and (C) electrooxidatively coated PVF, 5 × 5 μm.

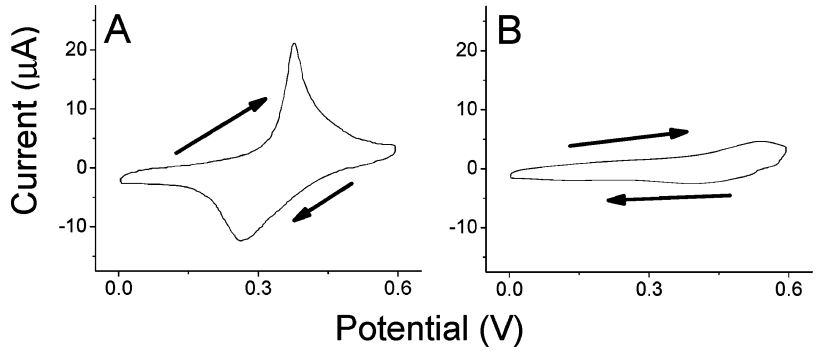

Figure 2. Cyclic voltammograms of electrooxidatively coated PVF at a scan rate of 50 mV/s: (A) film cycled in 0.1 M $NaClO_4$ and (B) film cycled in 0.05 M GGG.

co-ions (cation ejection) from the predoped neutral IL salt. This multistep doping/undoping mechanism allows us to explore two methods for IL-based conditioning of PVF films: (1) soaking PVF films in IL for 24 h and (2) potential cycling of PVF in IL at a scan rate of 50 mV/s between 0 and 0.6 V for 10 to 20 cycles. Recall that the goal here is to tune the original PVF films to achieve a state capable of transporting large ions like GGG^-. Although both methods were effective in tuning PVF to become more compatible with anion doping/undoping, the soaking method is quite time-consuming and lengthy. Soaking durations in certain ILs may result in partial PVF dissolution due to the multiplicity of interactions (e.g., hydrogen bonding, $\pi-\pi$, dipolar, ionic) possible between an IL and PVF. Therefore, potential cycling of PVF in IL was selected as the conditioning method to be used here.

Figure 3 shows the results of conditioning with the two ILs 1-*n*-butyl-3-methylimidazolium tetrafluoroborate ([BMIM][BF_4]) and *N*,*N*-methyl-*n*-butylpyrrolidinium bis(trifluoromethanesulfonyl)imide ([C_4mpy][Tf_2N]). [BMIM][BF_4] helped to open counterion conduits in the PVF matrix to some degree (panels A and B), resulting in a much more apparent anodic and cathodic peaks with a peak separation (ΔE) of 0.17 V. ΔE is the difference between the anodic peak potential (E_{pa}) and the cathodic peak potential (E_{pc}). Conditioning of a PVF film with another IL, [C_4mpy][Tf_2N], resulted in even greater compatibility with the GGG^- doping/undoping, resulting in a ΔE of 0.10 V (panels C and D). Additionally, the oxidation and reduction took place at considerably lower potentials. That is, E_{pa} decreased from 0.48 V for [BMIM][BF_4]-treated PVF to 0.30 V for [C_4mpy][Tf_2N]-treated PVF while E_{pc} decreased from 0.31 V for [BMIM][BF_4]-treated PVF to 0.20 V for [C_4mpy][Tf_2N]-treated PVF.

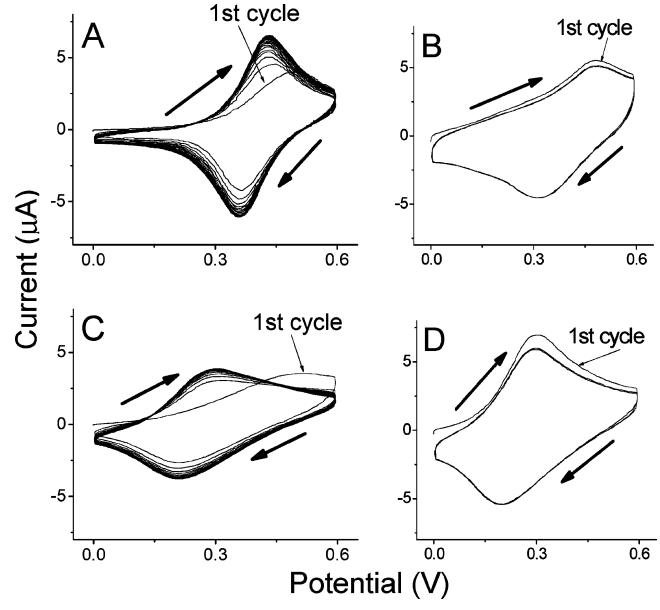

Figure 3. Cyclic voltammograms of electrooxidatively coated PVF with sufficient cycles recorded until a steady state was reached (scan rate = 50 mV/s): (A) in pure [BMIM][BF_4], 22 cycles; (B) in 0.05 M GGG after cycling in [BMIM][BF_4], 3 cycles; (C) in pure [C_4mpy][Tf_2N], 23 cycles; and (D) in 0.05 M GGG after cycling in [C_4mpy][Tf_2N], 3 cycles.

During the conditioning step, the shape of the anion plays an important role in mediating the interaction between the IL

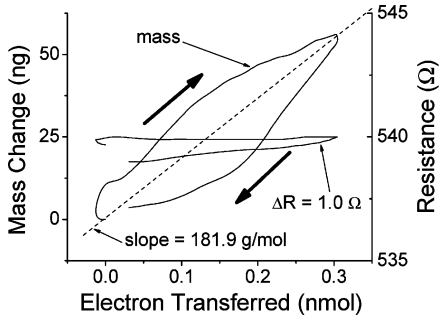

Figure 4. Mass change versus electrons transferred for GGG^- doping/undoping of a PVF film. Potential scan rate = 50 mV/s. Scan range = 0−0.6 V. The slope of the dotted line is 181.9 g/mol.

and the PVF-modified gold electrode. It has been suggested that the PVF matrix can be made compatible with certain anions so long as the polymer film is tuned with other species having similarly shaped anions.[8] Therefore, a plausible explanation for the current result is that $[C_4mpy][Tf_2N]$ gives better performance than $[BMIM][BF_4]$ in conditioning PVF for GGG^- doping/undoping because both $[Tf_2N^-]$ and GGG^- approximate rod-like shapes while $[BF_4^-]$ is roughly spherical.

An EQCM study revealed that for a $[C_4mpy][Tf_2N]$-conditioned PVF-modified electrode, during the doping/undoping process one GGG^- was involved for each electron transferred. Figure 4 shows how the PVF film mass changes with the amount of electron transfer. A small damping resistance (R) change of about 1 Ω (∼0.2%) suggests that the PVF film was rigid during GGG^- doping/undoping, which is critical in the following QCM calculation. The value of the mass change was obtained from QCM measurement. Specifically, for each 1 Hz of frequency decrease, the PVF film mass increased by 1.02 ng based on the calculation according to Sauerbrey's equation.[20] The amount of electron transfer was obtained from the charge (Q) in the electrochemical measurement. The slope of the fitted straight line (the dotted profile in Figure 4) was 181.9 g/mol. In other words, for each mole of electrons transferred from the PVF film to the gold electrode, the PVF film mass increased by 181.9 g. This result corroborates the fact that the mass increase was caused by the doping of GGG^-, which has a formula weight of 188.2 g/mol. That is, when PVF is oxidized, GGG^- enters the film to balance the excessive positive charge developed within the PVF matrix. Conversely, during PVF reduction, for each mole of electrons transferred from the gold electrode back into the PVF film, one mole of GGG^- leaves the polymer matrix to maintain electroneutrality.

3.2. Selective Conditioning and IL/PVF Interaction. When performing CV in ILs, the IL anion or perhaps both ions may be involved in doping and undoping.[8] The interaction between the IL components and the polymer matrix may be of a physical, mechanical, and/or chemical nature. Such treatment will potentially change the microstructure of the polymer matrix to accommodate the doping/undoping of species of interest.

With the extensive molecular diversity available among ILs, it is reasonable to suggest that the conditioning of PVF can be

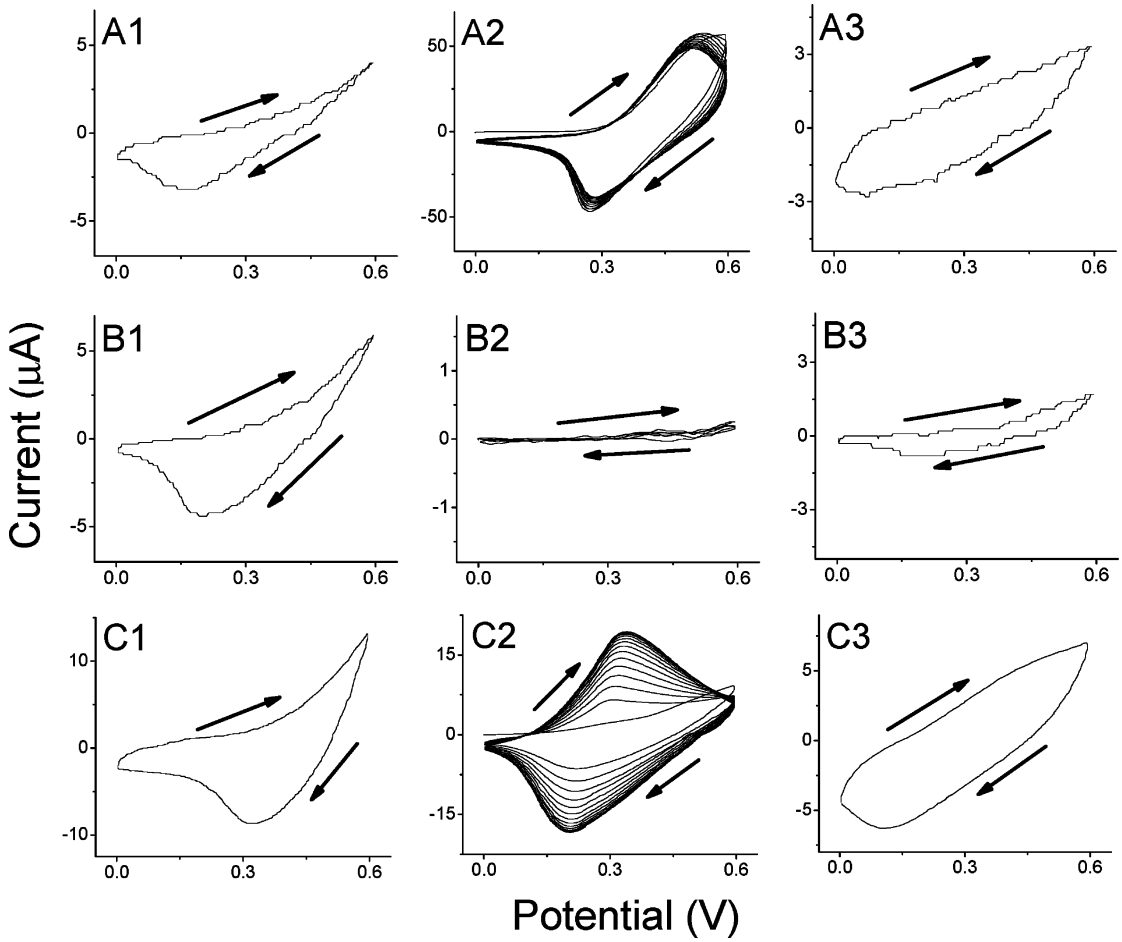

Figure 5. Cyclic voltammograms of electrooxidatively coated PVF at a scan rate of 50 mV/s: (column 1) in 0.05 M GGG prior to conditioning in IL; (column 2) in pure IL; (column 3) in 0.05 M GGG after conditioning in IL. The ionic liquid was $[BBIM][PF_6]$ (row A), $[N_{8888}][AOT]$ (row B), and [BMIM][beti] (row C).

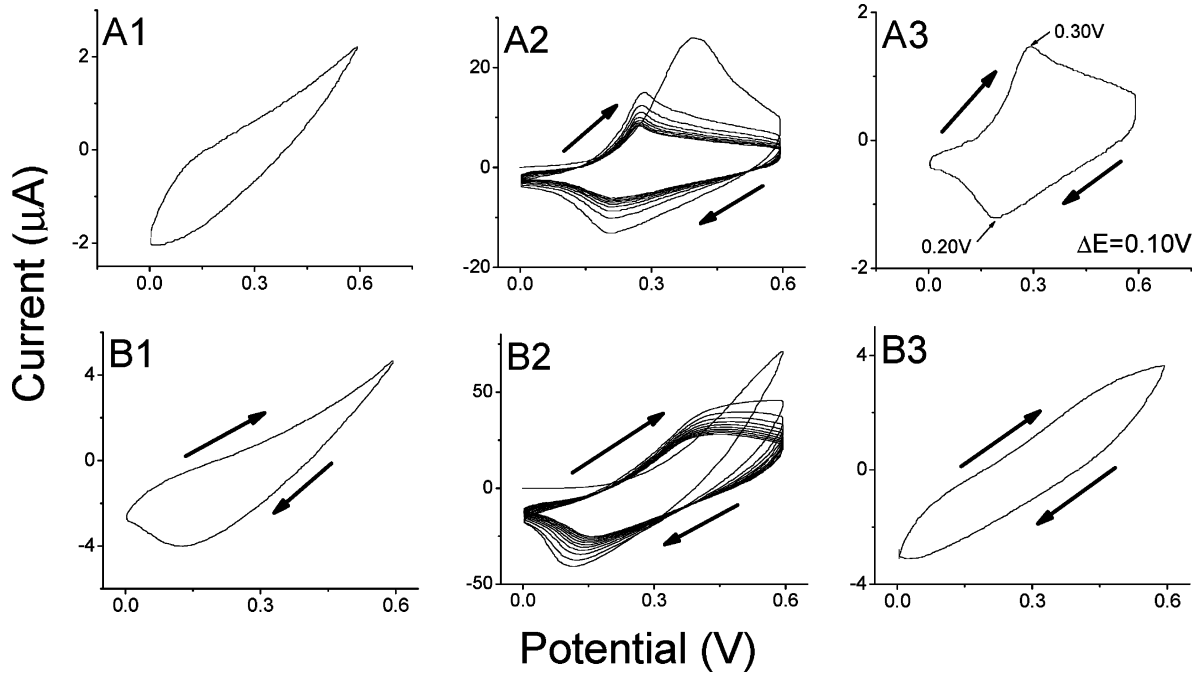

Figure 6. Cyclic voltammograms of electrooxidatively coated PVF at a scan rate of 50 mV/s: (column 1) in 0.05 M GGG before conditioning in IL; (column 2) in pure ILs; and (column 3) in 0.05 M GGG after conditioning in IL. The films were conditioned with $[C_5mpy][Tf_2N]$ (row A) and $[N_{3336}][Tf_2N]$ (row B).

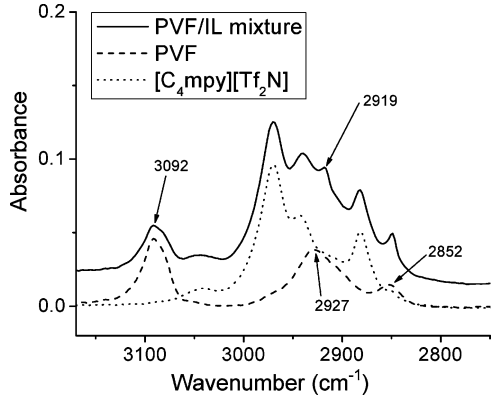

Figure 7. ATR-FTIR spectra of thin films: (A) pure PVF (dashed line), (B) pure $[C_4mpy][Tf_2N]$ (dotted line), and (C) 1:1 mixture of PVF and $[C_4mpy][Tf_2N]$ (solid line).

made fairly specific to the doping/undoping of desired anions based on the selection of task-specific ILs. For a treatment to be successful, two requirements must be met. One is that the IL should change the polymer microstructure to the correct form. Most likely, this will require that the anion of the IL have a shape similar to the anion of interest for targeted transport in the polymer. For example, the $[BF_4^-]$ anion has a spherical shape as does perchlorate, while the bis(trifluoromethanesulfonyl)imide ($[Tf_2N^-]$) anion is a bent rod, much more similar to GGG^-. The other requirement is that the IL must interact sufficiently with the polymer matrix. In addition, a practical issue emerges that some ILs may be much too viscous to penetrate the polymer matrix easily, despite the fact that their anions may be shaped similarly to the anion whose delivery is intended. Figure 5 shows several additional examples for conditioning by suboptimal ILs in which the above conditions are not fully met.

The potential was swept for several cycles for electrooxidatively coated PVF electrodes in $[BBIM][PF_6]$ (Figure 5, panel A2) and $[N_{8888}][AOT]$ (Figure 5, panel B2). The effectiveness of the IL/PVF interaction is reflected in the shape of the cyclic voltammograms and the magnitude of the current produced. The fact that $[BBIM][PF_6]$ interacts effectively with PVF can be seen since PVF was conditioned at 0.0 V before the redox cycling. At 0.0 V, both PVF and $[BBIM][PF_6]$ are hydrophobic, so significant interaction is expected. However, the spherical $[PF_6^-]$ anion cannot suitably modify the PVF microstructure for subsequent GGG^- doping/undoping (Figure 5, panels A1 and A3). On the contrary, the $[AOT^-]$ anion is somewhat rod-shaped as per GGG^-, but still cannot interact sufficiently with PVF owing to its excessive viscosity (Figure 5, panels B1 and B3).

In some other cases, such as for [BMIM][beti], the anions of the IL have the desired rod shape reminiscent of GGG^-, and the anions can dope/undope PVF films with reduced resistance after several cycles of "break-in" (Figure 5, panel C2). However, the GGG^- still cannot effectively dope into the PVF film effectively after treatment with [BMIM][beti]. It seems that the $[beti^-]$ anion does not have as strong an interaction with the PVF matrix as $[Tf_2N^-]$ and so the PVF matrix does not transform to a degree that GGG^- can dope/undope with little resistance (compare panels A3 and C3 in Figure 5).

Comparing cyclic voltammograms in column 3 to those in column 1 (Figure 5), it becomes obvious that the response of the PVF films in these cases is worsened after conditioning with ILs. This underscores the fact that ILs with improper size, functionality, or shape block conduits in the PVF polymer matrix to some degree, impeding the ability of the polymer to transport ions thereafter.

Additional results confirm that the nature of the IL anion is not the sole factor that determines the success of PVF conditioning. Indeed, the identity of the cation plays a key role. This supports our earlier conclusion that both cations and anions are involved in doping/undoping during potential cycling of PVF films in neat ILs.[8] To illustrate this concept, we tested two additional ILs for their ability to condition PVF films for GGG^- doping, $[C_5mpy][Tf_2N]$ and $[N_{3336}][Tf_2N]$. $[C_5mpy][Tf_2N]$, which contains a pyrrolidinium cation similar to that in

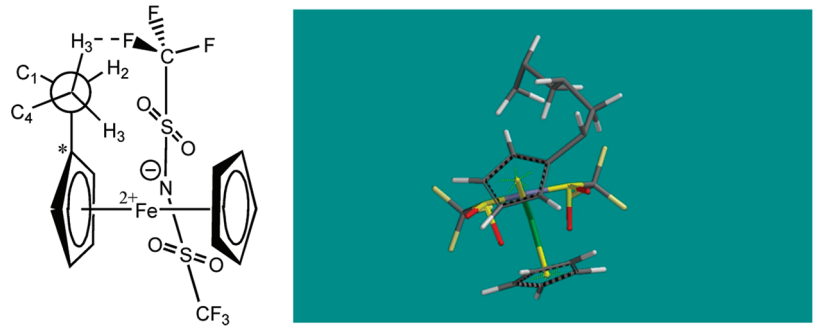

Figure 8. Proposed interaction between $[C_4mpy][Tf_2N]$ and PVF (left: schematic drawing; right: 3D representation generated with Spartan software). In the PVF structure, H_2 is the tertiary hydrogen and the two H_3 atoms are the hydrogen atoms of a methylene group. For ease of viewing, the aromatic hydrogen atoms on ferrocene are not explicitly shown.

$[C_4mpy][Tf_2N]$ (they simply differ in having a pentyl and butyl side chain, respectively), was similarly able to condition PVF with a proper microstructure for GGG^- doping/undoping (Figure 6, row A). In fact, by comparing panel A3 of Figure 6 with panel D of Figure 3, we find that the peak potentials and ΔE are virtually indistinguishable for PVF films conditioned with $[C_4mpy][Tf_2N]$ and $[C_5mpy][Tf_2N]$.

On the contrary, $[N_{3336}][Tf_2N]$ was unable to condition PVF for GGG^- doping/undoping despite the fact that this IL has the same $[Tf_2N^-]$ anion. Clearly, the dramatic difference between $[C_5mpy][Tf_2N]$ and $[N_{3336}][Tf_2N]$ must originate in the choice of cation. According to the cyclic voltammograms presented in Figure 6 (panels A2 and B2), $[C_5mpy][Tf_2N]$ either exhibits greater mobility than $[N_{3336}][Tf_2N]$ or the pyrrolidinium IL interacts with PVF with lower resistance than for the acyclic ammonium IL.

3.3. FTIR Results. Figure 7 highlights the C−H stretching portions of FTIR spectra for PVF, $[C_4mpy][Tf_2N]$, and a 1:1 mixture of the two.

In the ATR-FTIR spectrum of PVF, the peak at 3092 cm^{-1} can be ascribed to aromatic C−H stretching and the doublet at 2927 and 2852 cm^{-1} assigned to C−H stretching from the polymer backbone. When PVF is mixed with $[C_4mpy][Tf_2N]$, their interaction induces some noticeable changes to the PVF infrared absorption. The absorption at 2927 cm^{-1} shifts to a lower frequency of 2919 cm^{-1}, while the other absorption band at 2852 cm^{-1} remains virtually unchanged. If this red shift is associated with hydrogen bonding between a fluorine atom of $[C_4mpy][Tf_2N]$ and a hydrogen atom along the PVF backbone, it is likely that the methylene group is involved rather than the tertiary C−H bond. Indeed, the asymmetrical stretch of a methylene group usually occurs near 2926 cm^{-1} while the tertiary C−H stretching is displayed at about 2890 cm^{-1}.[21] The fact that the absorption at 3092 cm^{-1} barely changes suggests that the aromatic C−H groups are not heavily involved in the PVF/IL interaction.

Figure 8 illustrates the proposed interaction between $[C_4mpy][Tf_2N]$ and PVF, consistent with the FTIR observations described above. As the iron center carries positive charge and the extra positive charge is localized around iron during oxidation, we assume that the nitrogen atom of $[Tf_2N^-]$ anions has a strong interaction with the iron atom of PVF. In addition, the hydrogen bond basicity of ILs is largely determined by the identity of the anions;[22−24] therefore, we include only the anion of $[C_4mpy][Tf_2N]$ in the representation shown in Figure 8. In this view, the ferrocene axis cannot lie coplanar with the PVF backbone chain because of the conformational restriction at the carbon atom labeled with the asterisk in Figure 8. During interaction, the $[Tf_2N^-]$ anion aligns perpendicular to the ferrocene axis because of steric hindrance. In this configuration, one fluorine atom is then able to form a hydrogen bond with the methylene group of PVF.

4. Conclusions

Our reported results validate the concept that ILs can be used to fine-tune the structure of conductive polymers for the permselective doping and undoping of large ions under potentiodynamic electrochemical control. Reminiscent of molecular imprinting, the similarity in the structure, geometry, and chemical nature of the ions comprising the conditioning IL to the target ion clearly plays a vital role in the overall effectiveness of the conductive polymer conditioning step. In this work, $[C_4mpy][Tf_2N]$ and $[C_5mpy][Tf_2N]$ were found to effectively tune electrooxidatively coated PVF-modified electrodes for compatibility with subsequent GGG^- doping and dedoping. With the vast catalog of ILs available, it is reasonable to suspect that a particular task-specific IL can be identified or designed for the purpose of tuning conductive polymer structures for the optimum transport of a broad range of desired molecules. The ease and generality of this method suggest great promise for its use in various areas where conductive polymers are applied to (bio)analytical sensing, energy transduction materials, electromechanical actuators, and electrochromic or electroluminescent devices.

Acknowledgment. This research was supported in part by the Oakland University Research Excellence Fund and by the National Institute for Occupational Safety and Health. Dr. Yijun Tang is currently an assistant professor in the department of chemistry at the University of Wisconsin Oshkosh. G.A.B. was supported by the Office of Basic Energy Sciences, U.S. Department of Energy, under Contract DE-AC05-0096OR22725.

References and Notes

(1) Murray, R. W. *Annu. Rev. Mater. Sci.* **1984**, *14*, 145–169.
(2) Wallace, G. G.; Spinks, G. M.; Kane-Maguire, L. A. P.; Teasdale, P. R. *Conductive Electroactive Polymers*; CRC Press: Boca Raton, FL, 2003.
(3) George, P. M.; LaVan, D. A.; Burdick, J. A.; Chen, C.-Y.; Liang, E.; Langer, R. *Adv. Mater.* **2006**, *18* (5), 577–581.
(4) Hepel, M. *Electrochim. Acta* **1996**, *41*, 63.
(5) Seanor, D. A. *Electrical Properties of Polymers*; Seanor, D. A., Ed.; Academic Press: New York, 1982; p 6.
(6) Wegner, G. *Electronic Properties of Polymers and related Compounds*; Kuzmany, H., Mehring, M., Roth, S., Eds.; Springer-Verlag: Berlin, Germany, 1989; p 18.
(7) Wen, X.-M.; Wang, H.-Y.; Li, S.-L. *J. Chem. Res.* **2006**, *12*, 776–778.
(8) Tang, Y.; Zeng, X. *J. Electrochem. Soc.* **2008**, *155* (5), F82−F90.
(9) Baker, G. A.; Baker, S.; Pandey, S.; Bright, F. V. *Analyst* **2005**, *130*, 800–808.
(10) Daum, P.; Murray, R. W. *J. Phys. Chem.* **1981**, *85*, 389–396.

(11) Hillman, A. R.; Swann, M. J.; Bruckenstein, S. *J. Electroanal. Chem.* **1990**, *291*, 147–162.
(12) Yu, L.; Sathe, M.; Zeng, X. *J. Electrochem. Soc.* **2005**, *152* (11), E357−E363.
(13) Cooper, T.; Freeman, H. C.; Robinson, G.; Schoone, J. C. *Nature* **1962**, *194*, 1237–1239.
(14) Koleva, B. B.; Kolev, T. M.; Spiteller, M. *Biopolymers* **2006**, *83*, 498–507.
(15) Burrell, A. K.; Del Sesto, R. E.; Baker, S. N.; McCleskey, T. M.; Baker, G. A. *Green Chem.* **2007**, *9*, 449–454.
(16) Baker, S. N.; McCleskey, T. M.; Pandey, S.; Baker, G. A. *Chem. Commun.* **2004**, 940–941.
(17) Jin, H.; O'Hare, B.; Dong, J.; Arzhantsev, S.; Baker, G. A.; Wishart, J. F.; Benesi, A. J.; Maroncelli, M. *J. Phys. Chem. B* **2008**, *112* (1), 81–92.
(18) Bruckenstein, S.; Pater, E.; Hillman, A. R. *Anal. Chem.* **2000**, *72*, 1598–1603.
(19) Buttry, D. A.; Ward, M. D. *Chem. Rev.* **1992**, *92*, 1355–1379.
(20) Sauerbrey, G. *Z. Phys.* **1959**, *155*, 206–222.
(21) Silverstein, R. M.; Bassler, G. C.; Morrill, T. C. *Spectrometric Identification of Organic Compounds*, 5th ed.; John Wiley & Sons: New York, 1991.
(22) Hapiot, P.; Lagrost, C. *Chem. Rev.* **2008**, *108*, 2238–2264.
(23) MacFarlane, D. R.; Pringle, J. M.; Johansson, K. M.; Forsyth, S. A.; Forsyth, M. *Chem. Commun.* **2006**, *18*, 1905–1917.
(24) Sarkar, A.; Trivedi, S.; Baker, G. A.; Pandey, S. *J. Phys. Chem. B* **2008**, *112*, 14927–14936.

JP1030202